The NASA Seasonal-to-Interannual Prediction Project (NSIPP)

NASA Goddard Space Flight Center

Progress Report

July 20, 2001

The NASA Seasonal-to-Interannual Prediction Project (NSIPP)
Annual Report for 2000

GOAL

To develop an assimilation and forecast system based on a coupled atmosphere-ocean-land-surface-sea-ice model capable of using a combination of satellite and in situ data sources to improve the prediction of ENSO and other major S-I signals and their global teleconnections.

OBJECTIVES

Demonstrate the utility of satellite data, especially surface height surface winds, air-sea fluxes and soil moisture, in a coupled model prediction system.

Aid in the design of the observing system for short-term climate prediction by conducting OSSE's and predictability studies.

http://nsipp.gsfc.nasa.gov

Principal Investigator: Michele Rienecker, Code 971

Co-Investigators: Max Suarez, Code 913
David Adamec, Code 971
Randal Koster, Code 974
Siegfried Schubert, Code 910.3
James Hansen, Code 940

Funded by NASA/ESE: Global Modeling and Analysis Program
Physical Oceanography Research and Analysis Program.

The NASA Seasonal-to-Interannual Prediction Project (NSIPP) Annual Report for 2000

Table of Contents

Summary Highlights 1

Background 1

1. CGCM Experiments 3

2. Forecasts 6
   2.1 CGCM Forecast (Tier 1) 6
   2.2 AGCM-LSM (Tier 2) Forecasts 11

3. Predictability Studies 12
   3.1 Tier 2 Predictability Studies 12

4. Coupled AGCM-LSM Experiments 15

5. Ocean Data Assimilation 18
   5.1 Introduction 18
   5.2 MvOI Tests 18
   5.3 Ensemble Kalman Filter Tests 20
   5.4 Results From the Multivariate Assimilation of Satellite Altimetry 23

6. Land Assimilation 24

7. Other Investigations 24
   7.1 Subtropical-Tropical Ocean Exchanges 24
   7.2 ENSO Dynamics 25
   7.3 Atmospheric Equatorial Momentum Budget 25

8. Model Development 26
   8.1 AGCM Development 26
   8.2 LSM Development 27

References 28

NSIPP Personnel 29

NSIPP Publications, 2000 30

Model Data Distribution 32

NSIPP Science Team 33

NSIPP Associate Investigators 33

Summary Highlights

CGCM simulations: Simulations have been conducted with the updated atmospheric model (NSIPP1 AGCM). Interannual variability is strongly biennial. Sensitivity experiments were conducted to test the impact of MJO variations on the amplitude and period of ENSO variations with little improvement.

Tier 1 Forecasts: Implemented 9-member ensemble forecasts; routine forecasts conducted monthly.

Tier 2 Forecasts: Routine ensemble forecasts conducted monthly over Tier-1 forecast SST and IRI consensus SST forecast. The latter are contributed to IRI multi-model consensus forecast.

Predictability Studies: Large ensembles of AGCM-LSM experiments demonstrate potentially predictable differences between the extratropical response to 1982/83 and 1997/98 El Niños. The main predictable signal of the 1988 drought and 1993 floods in the U.S. is associated with memory of the initial soil moisture anomalies that developed during the previous winter and spring.

AGCM-LSM Experiments: An LDAS-style experiment run in coupled mode demonstrates that a more realistic soil moisture boundary condition improves the model's precipitation.

Ocean Data Assimilation: Tests conducted for assimilation of altimetric data with multivariate optimal interpolation and Ensemble Kalman Filter. Long assimilation runs with temperature-only assimilation highlight problems if salinity is not adjusted.

AGCM development: NSIPP1 AGCM frozen. Development begun on NSIPP2, including implementation of a prognostic cloud liquid water scheme and the new catchment LSM.

LSM development: Tests of the catchment model have continued. Other developments have focused on the improvement of a physically - based photosynthesis and stomatal conductance parameterization as a step towards dynamic vegetation.

AGCM Simulations: Nine-member ensemble AMIP simulations have been run for 70 years with the NSIPP1 AGCM. These have been made available to the community through the internet.

Background

Understanding and predicting seasonal-to-interannual climate variations is an essential goal within the overall NASA strategy for climate research. The NASA Seasonal to Interannual Prediction Project (NSIPP) has been established as a core research and development activity at the Goddard Space Flight Center (GSFC) to develop the use of existing and planned remote observing systems together with in situ observations for experimental predictions of seasonal-to-interannual climate variations. By focusing on the application of remotely sensed observations,

NASA expects to make unique contributions to the USGCRP, CLIVAR and GEWEX international research programs.

The NSIPP approach is based on the premise that coupled ocean-atmosphere-land general circulation models (CGCMs) offer the best prospect for predicting tropical sea surface temperature (SST) anomalies and of extending the prediction of global precipitation and temperature anomalies. The NSIPP CGCM is comprised of the NSIPP1 atmospheric model, the Poseidon quasi-isopycnal ocean model and the Mosaic land surface model (LSM), all developed at Goddard. The key to tropical forecasts lies in initialization of the upper ocean, and the key to summertime precipitation forecasts over the continental U.S. lies in the initialization of soil moisture; therefore, ocean and land surface data assimilation are essential elements in NSIPP's strategy.

The NSIPP CGCM and ocean data assimilation system have been implemented on a scalable parallel architecture _ currently, a T3E parallel system with 1024 nodes. This environment allows finer resolution global simulations than have been used previously for climate prediction. Coupled simulations are run routinely at 2 degrees for the atmosphere and 2/3 degree for the ocean, and finer resolution models _ ranging from 0.5 degree for the atmospheric GCM and 1/3 degree for the ocean _ are being run experimentally. The use of ensembles, in both simulations and assimilation/forecasts, is integral to NSIPP's approach.

NSIPP produces routine experimental ENSO predictions of SST for the tropical Pacific region by assimilating TAO temperature observations. The SST from these predictions is used to force coupled atmosphere-land ensemble predictions. Ensembles allow the characterization of the uncertainty of the forecasts, so that categorical forecasts are also presented on the web.

In the coming year we expect to assess the utility of remotely-sensed sea surface height for initializing the tropical oceans for coupled predictions. In addition to global assimilation of surface altimetry, we will expand the situ temperature assimilation to include the global XBT and other in situ databases. A scheme has been implemented to correct salinity with temperature so that long assimilations will be conducted with a simple univariate OI. We will continue to use SSM/I - based surface wind analyses for ocean initialization and plan to assess the added value of TRMM precipitation products and of the high resolution vector winds from QuikSCAT. We will also investigate how to make best use of remotely-sensed soil moisture from SMMR (and, when available, AMSR) within the framework of the NSIPP Catchment land surface model.

NSIPP will continue to examine the predictability of El Niño and other major climate variations on seasonal-to-interannual time scales and the predictability of extra-tropical signals at these time-scales. The decadal modulation of predictability will also be examined. In the future it is anticipated that models with high resolution in specific areas will be used to investigate the downscale impact of large scale tropical SST anomalies.

Summary of Activities, January 2000 - January 2001

1. CGCM Experiments

The current implementation (Version 1) of NSIPP's coupled general circulation model (CGCM) uses the NSIPP atmospheric model developed by Suarez and Bacmeister, the Poseidon quasi-isopycnal reduced gravity ocean model developed by Schopf, and the Mosaic Land Surface model developed by Koster and Suarez. The CGCM is freely coupled, i.e., flux corrections are not employed. The seasonal cycle in SST along the equatorial Pacific, noted as deficient in the earlier coupled simulations was improved markedly with some parameter adjustments in the atmospheric surface boundary layer, by increased resolution at the top of the boundary layer, by reformulation of the re-evaporation, and by judicious filtering of topography. Below are results from recent coupled simulations, including an exploration of the influence of uncoupled atmospheric noise on the ENSO period, conducted in collaboration with Duane Waliser (SUNY).

A baseline simulation (EXP_HI) was conducted with an AGCM resolution of 2°x2.5°x34 layers, an OGCM resolution of 1/3°x5/8°x20 layers and about 15,000 tiles for the land surface model LSM. The OGCM was initialized from a forced ocean-only simulation, the AGCM-LSM from an AMIP-style simulation over Reynolds SST. The results presented here are from the last 20 years of a 40-year integration. EXP_LO has an AGCM resolution of 3°x3.75°x34 layers and OGCM resolution of 0.5°x1.25°x20 layers. Since the NSIPP CGCM simulation has very low energy at intraseasonal periods, a third experiment was conducted: EXP_LO_MJO has additional surface stress forcing over the equatorial ocean (10°S-10°N). Perturbations in the 35-100 day spectral band were superposed on the forcing applied to the ocean from the AGCM.

The model climatology

The model bias for EXP_HI, estimated from the mean drift in SST away from the Reynolds climatology over the last 20 years of the integration is presented in Figure 1. The drift is less than 1°C over much of the global tropics. Errors over 4°C along the west coasts of both South America and Africa are undoubtedly partly associated with inadequate low-level stratus. However the errors also appear to be related to the orientation of the surface stress near the land sea boundaries. Current investigations are exploring sensitivity to these stresses and ways to (a) ensure that the ocean is forced by appropriate marine stresses and fluxes, and (b) ameliorate the influence of steep mountain slopes on stresses near the land-sea boundary. The cold bias in the mid-latitudes may be the result of high cloudiness during summer. The larger errors in the Atlantic Ocean seem to be a pervasive feature of CGCMs.

The distributions of the mean and standard deviation for SST and zonal stress are presented in Figures 2 (a) and (b). The large scale distribution of SST is quite good, although there are some obvious discrepancies from observations: the warm pool extends too far east and the cold tongue

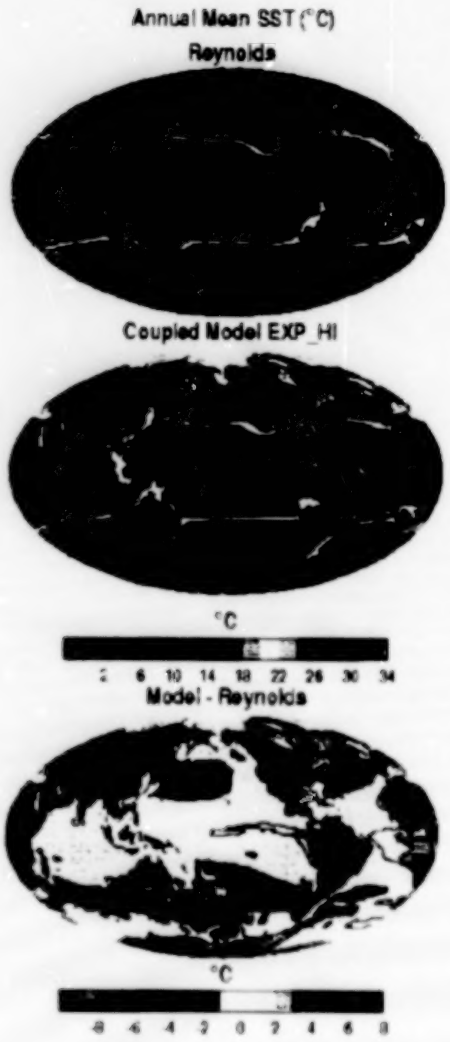

Figure 1: Annual mean SST from Reynolds (upper panel) and from the EXP_HI coupled simulation (middle panel). The contour interval is 2°C. The model bias, estimated as the deviation from Reynolds, is shown in the lower panel. The contour interval is 1°C.

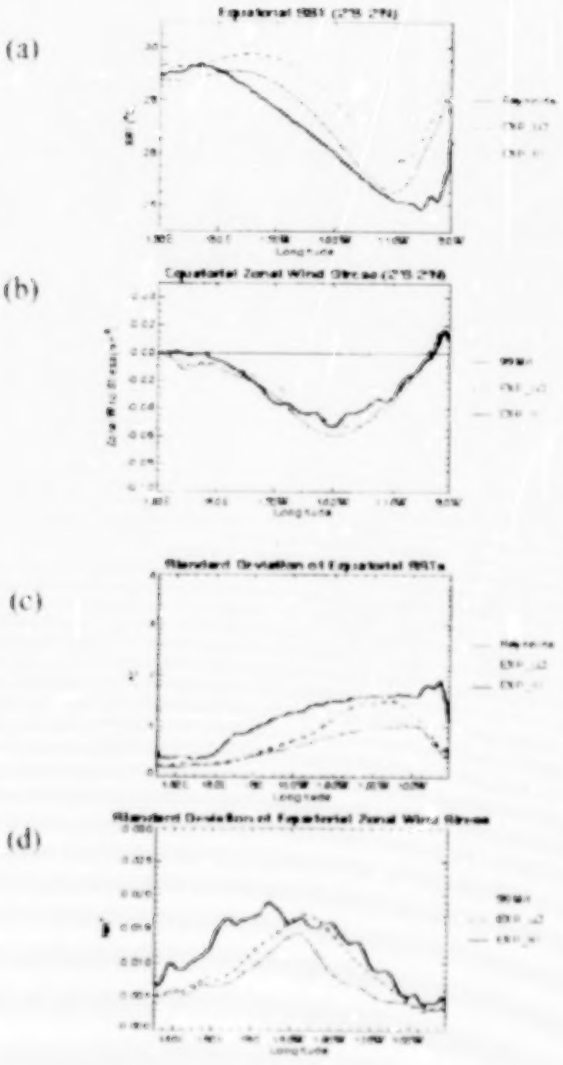

Figure 2: Annual mean (a) SST and (b) zonal stress and variance in (c) SST and (d) zonal stress along the equator from observations and from the coupled simulations.

terminates prematurely in the east. The zonal stress distribution is in excellent agreement with observations. The mean zonal stress does not differ as markedly between the simulations, although the mean stress is weaker for the lower resolution, and the region of strongest stress is shifted about 20° to the east.

The seasonal cycles of SST and zonal surface stress along the equatorial Pacific from EXP_HI compare reasonably well with Reynolds SST and surface stress estimated from the SSM/I analyses (Figure 3), although the amplitude of model SST is too weak. The semi annual signal

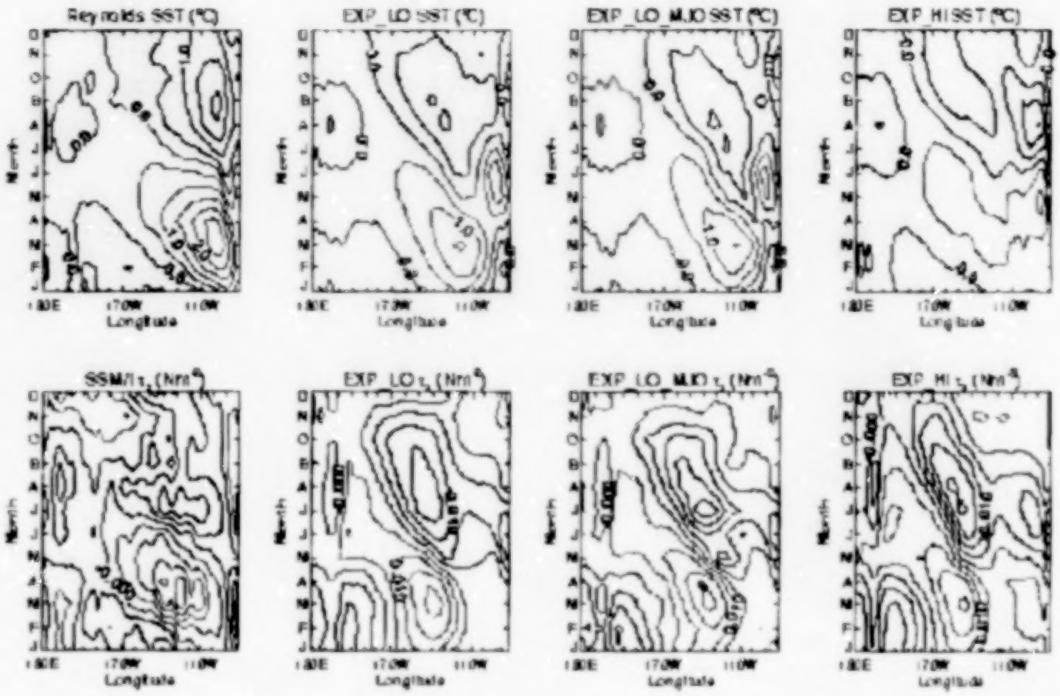

Figure 3: Seasonal cycle of SST (upper panels) and zonal wind stress (lower panels). Left hand column shows observations, other columns show the coupled simulations. Negative anomalies are shaded.

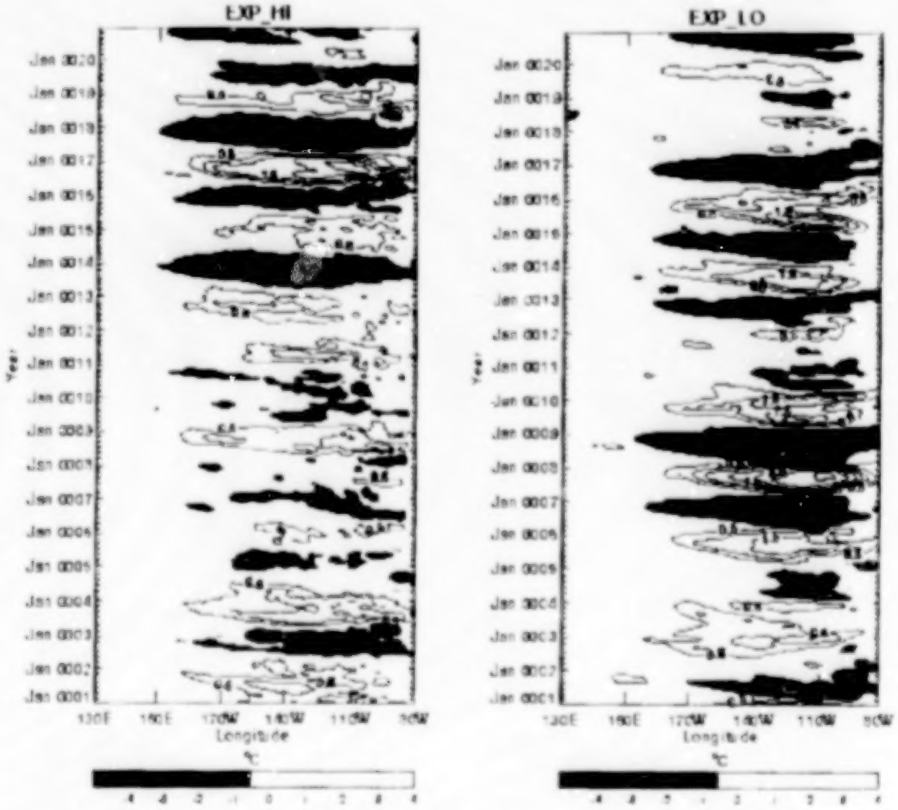

Figure 4: Interannual SST anomalies along the equatorial Pacific from the EXP_HI simulation (left) and the EXP_LO simulation (right). The dark shades are used for negative anomalies.

in zonal stress is too strong in the western Pacific and too weak in the central Pacific. The variations in the central-east are centered slightly west of SSM/I, with too strong westward phase propagation in the second half of the seasonal cycle. All the simulations remain deficient in the phasing of the zonal stress at both the western and eastern boundaries.

Interannual anomalies along the equator
The interannual SST anomalies along the equator from EXP_HI are weak, with maximum anomalies of about 2.5°C during the 20-year simulation (Figure 4). The interannual anomalies from the lower resolution simulations reach up to 3.5°C. The strongest anomalies tend to propagate eastward during the latter half of the event in EXP_LO. The stronger anomalies penetrate almost to the eastern boundary.

One of the most difficult characteristics of ENSO to simulate with CGCMs appears to be its irregularity. Most coupled simulations appear to have too strong a quasi-biennial signal and too weak quasi-quadriennial variability, and such is the case with these simulations. Two possible sources of ENSO irregularity are deterministic chaos within the nonlinear coupled system and uncoupled weather noise. The influence of uncoupled variability at timescales of 35-100 days was explored by merely adding the signal from Atlas's SSM/I surface stress at these scales, related to the Madden-Julian Oscillation, to the surface forcing provided to the ocean component of the CGCM. However, the interannual variability in SST was not markedly different from EXP_LO with this extra forcing and is not shown. The seasonal cycle apparently exerts a strong control on interannual variations in this CGCM.

2. Forecasts

2.1 CGCM Forecast (Tier 1)

During the first part of this year a series of experiments designed for assessing the impact of data assimilation of TAO temperatures on our forecasting system was completed. These experiments were conducted with the CGCM V0, i.e., with the previous version of the AGCM. The preliminary result that was reported last year, i.e., a significant increase in forecasting skill due to inclusion of TAO data, was confirmed. The next step in the development of this system was the introduction of ensembles of forecasts. Similar to what is done by other groups, the ensembles are produced by initializing the coupled model every 3 days around the beginning of every month: each ensemble contains 9 members. In this way the ocean model initial state is perturbed by including observed information over slightly different time periods. These experiments together with the inclusion of new cases led to the detection and correction of several technical problems in the initialization of the coupled model and in the assimilation code. These modifications led to a qualitatively different mean drift of the coupled model and we had to repeat the hindcasts from 1993 to 1999 in order to compute the new drift and then to resume our routine forecasts. Results from the new hindcast experiments starting around December 1 are presented followed by the December 2000 forecast that indicates the return of warm conditions in the tropical Pacific for 2000-2001.

Hindcasts of the Niño 3 SST anomalies from 1993 to 1999 are presented in Figure 5. During this period the model was initialized every 15 days (e.g., November 15, December 1 and December 15). A mean drift was computed over experiments starting in 1993 to 1995. The mean drift was then interpolated to each start date of the routine forecast (e.g., November 21, 24, 27, 30,

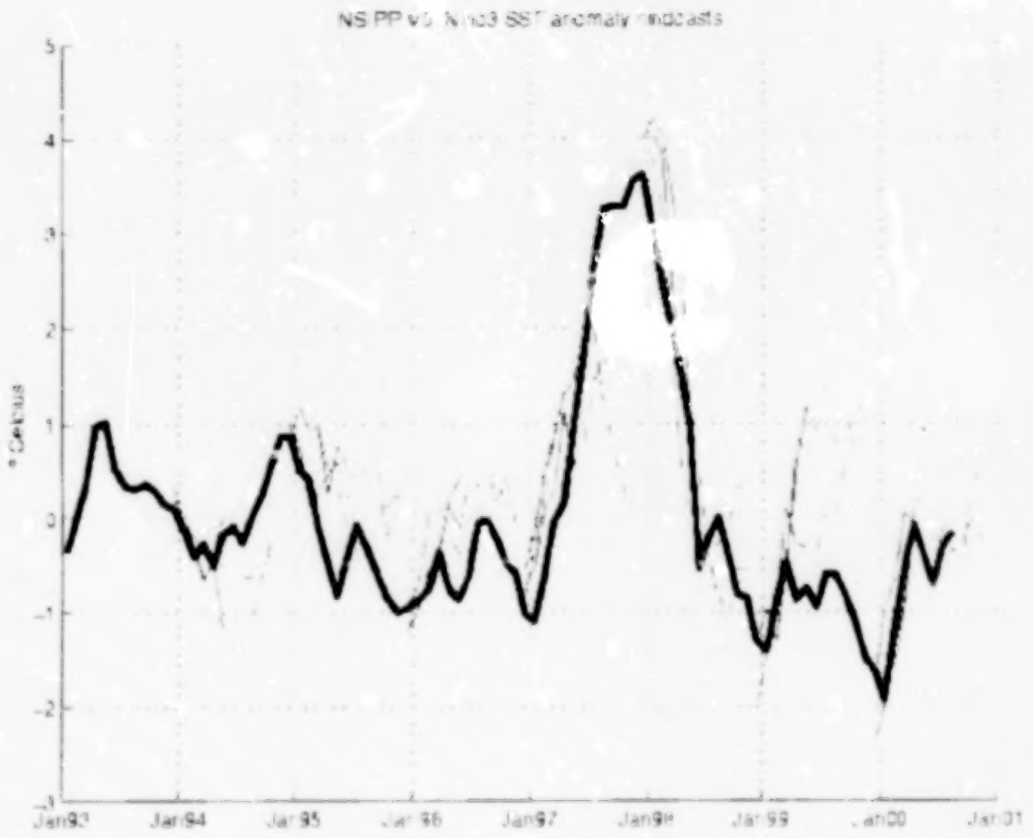

Figure 5. Hindcast Niño 3 SST anomalies compared with the Reynolds observations. The mean annual state is computed over 1993 to 1995. The blue, red and green lines correspond to experiments starting on November 15, December 1 and December 15 respectively. Solid lines represent 6-month hindcasts, dashed are 12-month hindcasts.

December 3, 6, 9, 12, 15) for the computation of interannual anomalies. Six-month forecasts are distinguished from 12-month forecasts. The former period is generally accepted as an easy test where most of the forecast models present a relatively good skill, the 12-month forecast being a harder target in terms of ENSO prediction. The model generally verifies well against observed temperature anomalies in the 6-month forecast. For example, the 1997-1998 ENSO event could have been captured from at least December 1996, and the decline of this event starting from December 1997 is remarkably well represented. This decline is explained by the arrival at the surface in the eastern Pacific of cold temperature anomalies originating subsurface in the western Pacific.

The only significant failure comes from experiments initialized from December 1998 when there was a false alarm for a warm episode in two out of three ensemble members. For the 12-month forecasts, all three ensemble members starting in December 1998 fail, i.e., produce a false warm forecast. Additionally, one ensemble member from the December 1999 forecast produced a false alarm for a warm event. Further, only one member continued to warm up after May 1997 for experiments starting in December 1996 while the two other members returned quickly towards neutral conditions.

One possible explanation for the false warm ENSO forecast from the December 1998 hindcast is based on the dominant quasi-biennial periodicity of the freely-run coupled model. Indeed, such a periodicity means that a cold year, e.g., 1998, should be followed by a warm year. This unrealistic feature of the model (the dominant periodicity in nature is quasi-quadrennial), can obviously lead to false cold or warm alarms. An explanation for the quasi-biennial periodicity of the model is that temperature anomalies in the eastern Pacific surface occur with opposite sign anomalies in the western Pacific subsurface. The latter propagate rapidly eastward and reverse the sign of eastern Pacific surface anomalies. The evolution of subsurface temperature anomalies for the hindcast starting November 15, 1998 is presented in Figure 6. It is clear that the erroneous warming in the eastern Pacific is the result of the positive temperature anomalies that first appear in the eastern Pacific subsurface, rather than in the western Pacific. Therefore, the hypothesis of quasi-biennial ENSO periodicity as the source of false alarms can be rejected for this particular case.

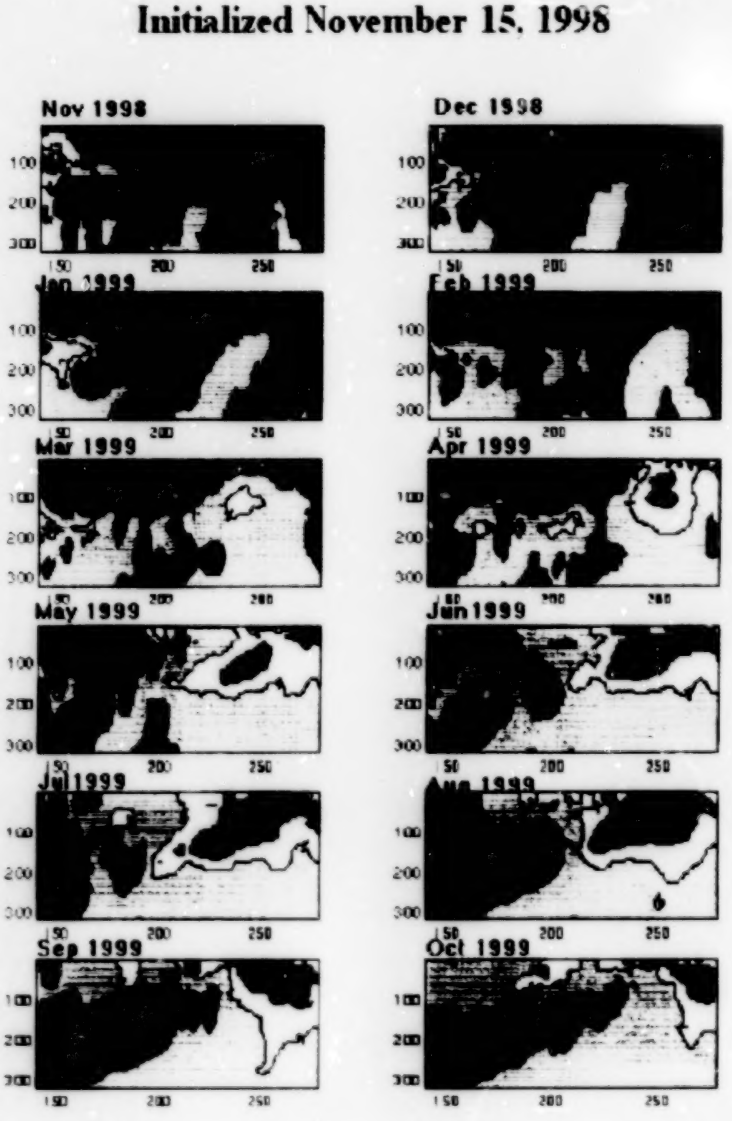

Figure 6. Monthly averaged temperature anomalies in the equatorial plane for the hindcast initialized on November 15, 1998.

For other cases, the evolution of anomalies in the eastern Pacific (rather than the size of the initial anomalies in the western Pacific) also lead to hindcast states that differ from observations. For the hindcast initialized in December 1996, the subsurface evolution of temperature anomalies along the equator for experiments starting November 15 and December 15, 1996 diverged after six months (not shown). During the first six months of the hindcast, both experiments displayed an eastward propagation of warm subsurface anomalies consistent with the observed onset of the 1997-1998 El Niño. After the sixth month, warm eastern Pacific anomalies attenuate while they continue to develop in the second. Differences between experiments starting in December 1999 are also explained by attenuation or increase of the temperature signal in the eastern Pacific.

It must be stressed that hindcasts starting in December present an inherit difficulty: they cross the spring predictability barrier. It is therefore possible that the non-predictable sign of air-sea feedback in the eastern Pacific is of natural origin. However, it is also possible for this behavior to be a result of interactions between the drifting mean state of the coupled model and forecast interannual anomalies. Completion of this set of experiments with initialization from each calendar month will allow the resolution of this question.

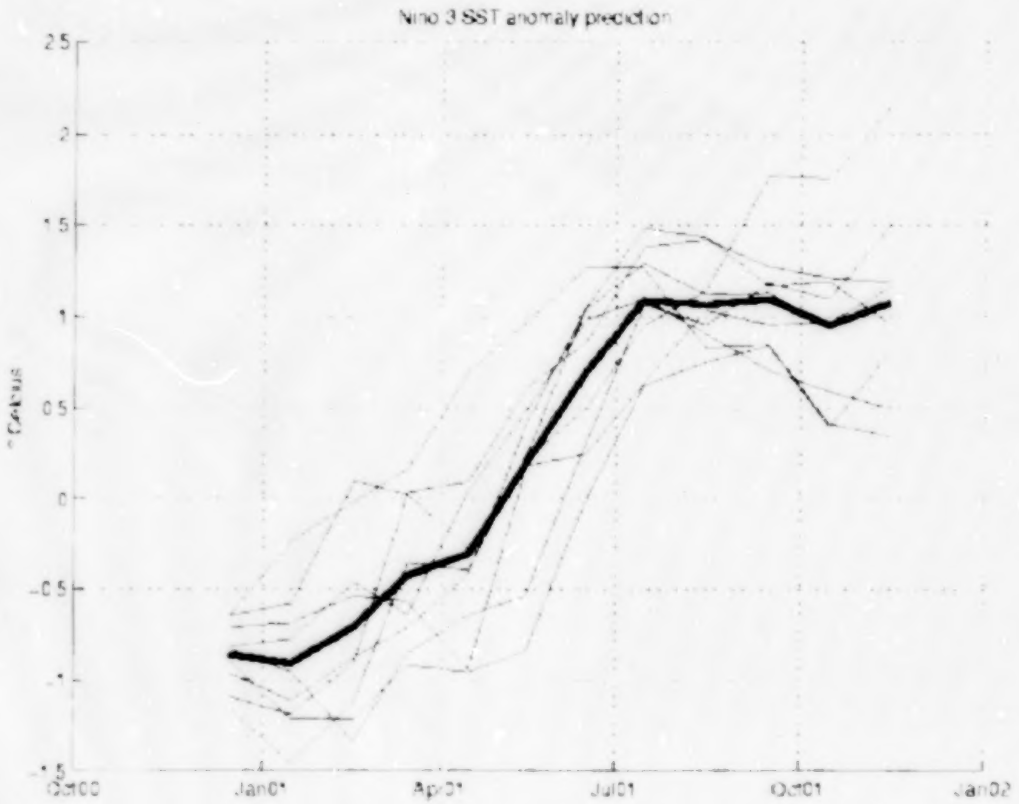

Figure 7. Forecast Niño 3 SST anomalies for experiments starting from November 22 to December 15, 2000. The thick black line is the ensemble mean

The forecast initialized in December 2000

The Niño 3 sea surface temperature anomalies forecast by the NSIPP CGCM V0 for initial conditions from November 21 to December 15, 2000 are shown in Figure 7. Ensemble averaged

subsurface anomalies are shown in Figure 8. The cold conditions present in the initial state end around May 2001 due to the arrival of warm anomalies from the western Pacific. The last part of the forecast (from May to November) shows the development of warm conditions. However, only one member of this ensemble indicates a continuous increase of the temperature anomalies. The rest indicate either stable or decreasing anomalies after July 2001. This behavior is repeated in forecasts initialized in January 2001. The next step is to undertake coupled forecasts with the updated AGCM in the coupled configuration, CGCM V1, and with improved oceanic initialization.

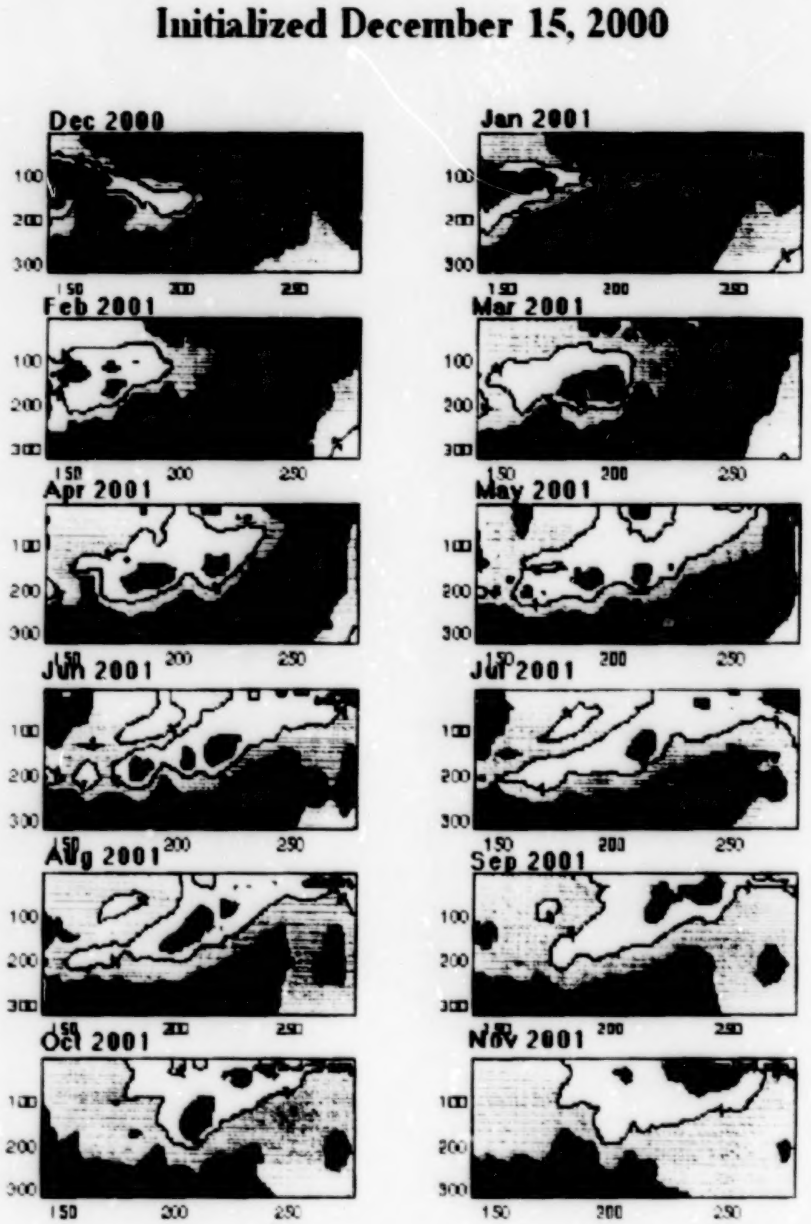

Figure 8. Monthly averaged temperature anomalies in the equatorial plane for the hindcast initialized on December 15, 2000.

2.2 AGCM-LSM (Tier 2) Forecasts

Two sets of Tier 2 forecasts are now produced routinely every month and posted at our web site. Each is an ensemble of four-month runs of the atmosphere-land model using prescribed, forecast SSTs. The two sets are conducted with NSIPP and NCEP Tier 1 forecast SST respectively. The latter set is comprised of 9 ensemble members and are contributed to the IRI quarterly multi-model consensus forecast. Atmospheric and soil initial conditions are taken from 9 on-going AMIP-style runs beginning at the middle of the month prior to the start of the SST forecast period. The Tier 2 forecasts carried out with the NSIPP Tier 1 forecast SSTs use atmospheric

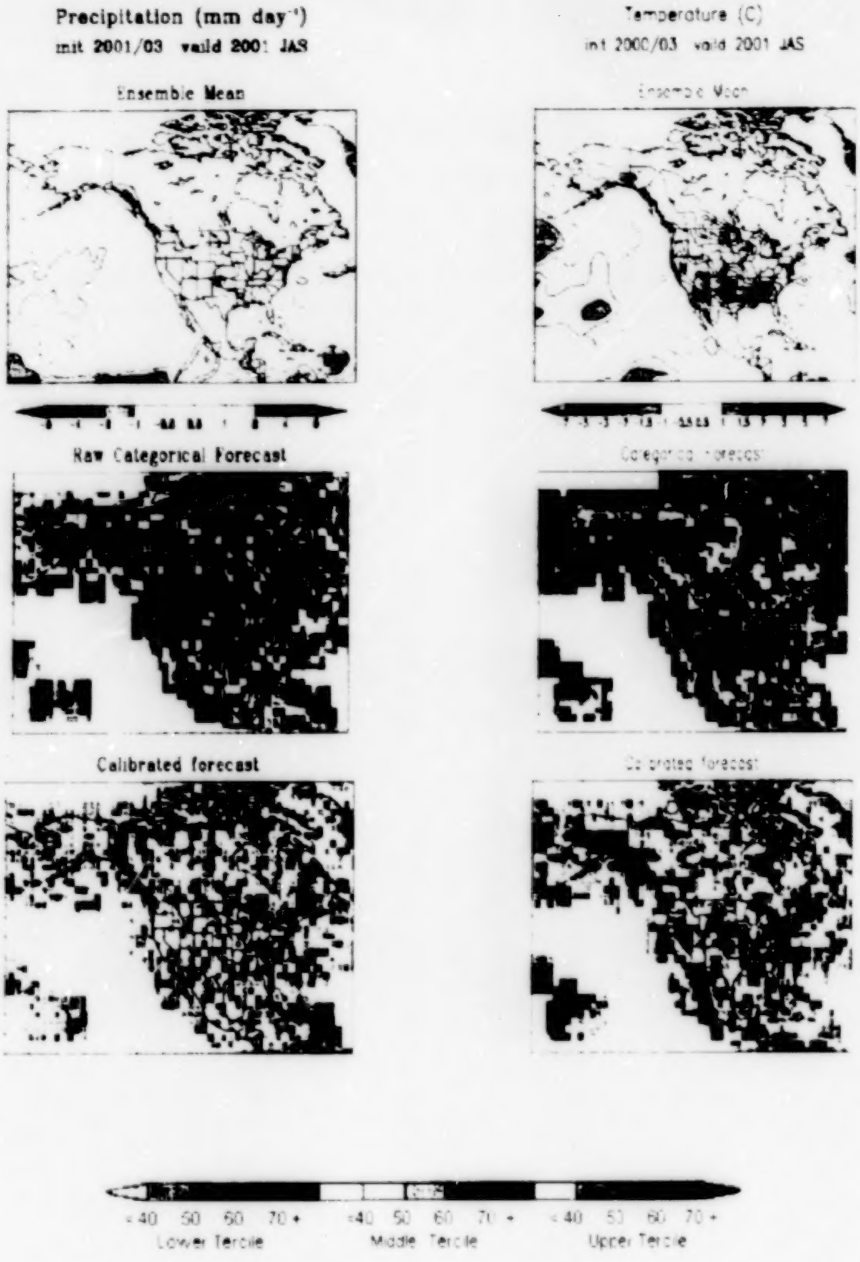

Temperature and precipitation anomalies from the member 18 ensemble mean. Anomalies are referenced to the 1980-1999 model climatology. Units are mm/day. Shaded values represent significance at the 95% confidence level of a two sided t-test.

The raw categorical forecast is based on the individual ensemble member's departure from the model climatology. The three categories are above (red), normal (gray), and below (blue). The category holding the most ensemble members is colored for each grid cell. The number is percentage of the ensemble members that fall into this category.

The calibrated categorical forecast based on past performance of the AGCM. Red is above normal, gray is normal and blue is below normal. Areas with no forecast skill are white. Numbers represent probability in percent that forecast will verify.

Figure 9. Tier 2 forecast of JAS 2001 precipitation (left column) and surface temperature (right column) initialized in March 2001.

initial conditions from a superposition of anomalies from the NCEP reanalysis at the middle of the month with the NSIPP model climatology. Nine ensemble members are generated by running the model over the 9 different SST forecasts. Land conditions (soil wetness, ground temperature, etc.) are the same for all nine runs and are taken from an AMIP-style run.

The NSIPP Tier 1 forecast SSTs are global, except for coastal areas and the Arctic. We take the NSIPP forecast directly, using zero anomalies where they are not defined. For the NCEP Tier 1 forecast SSTs, global SST anomalies are formed by combining the NCEP forecast between 25°S and 30°N, and 120°E and 70°W. The initial anomalies are damped with a 3-month exponential damping time outside this region.

For both NCEP and NSIPP, global anomalies are then added to a 20-year (1980-1999) SST climatology constructed from a combination of Reynolds and Hadley SST data. In both cases climatological sea-ice conditions are used.

The recent forecast for JAS 2001 mean surface temperature and precipitation initialized in March 2001, is presented in Figure 9. The use of an ensemble provides a mechanism for assessing statistical significance as well as forecast model validation. This information is provided for surface temperature and precipitation in the form of raw and calibrated categorical forecasts.

3. Predictability Studies

3.1 Tier 2 Predictability Studies

The ensemble AGCM-LSM experiments conducted are in two categories - AMIP-style experiments run continuously over observed SST for many years/decades or shorter (seasonal) experiments re-initialized each season. To date 9 AMIP-style ensemble integrations have been carried out for 1930-1999. Nine-member DSP ensembles have been conducted for each season for 1980-1999 and 36 ensemble members for the 1988 and 1993 boreal winters. Results from all of these experiments, including downloadable data files, are available from our web site.

Predictability and Forecast Skill for Boreal Winter

A substantial effort was made to characterize the predictability and forecast skill from the boreal winter DSP runs mentioned above. These results are published in a technical memorandum (Pegion et al. 2000) and are summarized here.

The report presents a comprehensive analysis of predictability and forecast skill for boreal winter. Results are based on the 20 (1980-1999) ensembles of nine January-February-March (JFM) hindcasts. The runs are forced with observed sea surface temperature (SST) and sea ice. The quantities examined are the global 200mb height, precipitation, sea level pressure, and North American surface temperature. The analysis shows that the NSIPP1 AGCM produces very realistic January-February-March (JFM) mean interannual variability. Comparisons with several other AGCMs demonstrate that the NSIPP model is state-of-the-art. The comparisons also show that there is a wide range among the models in the signal-to-noise ratios (SNRs), with the NSIPP1 model producing SNRs in the extratropics that are higher than most of the other models.

The results further show that the potentially predictable signal in the extratropics is predominantly associated with ENSO. The wave-like ENSO response emanates from the central and eastern tropical Pacific and, in the Northern Hemisphere, extends across much of the North Pacific Ocean and North America. The latter two regions are characterized by some of the largest extratropical signal-to-noise ratios with, for example, maximum values exceeding 5 for the 200mb height field during the ENSO years.

The noise in the 1983 and 1989 JFM forecasts was also re-examined to investigate the role of the basic state. The results corroborate those obtained in our previous study based on the GEOS-2 model (Chang et al. 2000)

The report presents various probabilistic verification measures that provide further indications of the reliability of the AGCM hindcasts. These include reliability diagrams, and various model probability density functions (pdfs) that help to determine whether the observations fall within the range of model solutions.

Are differences between EL Niños predictable?
As a first step toward understanding the sensitivity of the ENSO response to the details of the SST anomalies, a statistical analysis of the differences in the atmospheric responses during the two major warm episodes (1983 and 1998) was conducted. The report also presents our initial comparison of the two events using larger ensembles. The results suggest that there are potentially predictable differences in the extratropical response for these two extreme events. A key question that is addressed is whether the differences can be explained as a simple linear response to differences in the amplitude of the Niño3 SST anomalies during these two years.

Predictability of Zonal Means During Boreal Summer
The analysis focused on the 20 ensembles of nine boreal summer hindcasts (1980-1999). These runs were initialized in mid-May and ran through the end of August. The SST and sea ice were prescribed from observations. The atmospheric initial conditions were taken from the NCEP/NCAR reanalysis, while the initial soil moisture for each ensemble was taken from the appropriate year of one of our 20-year AMIP runs described above. During June-July-August (JJA) the predictability of the seasonal mean height field is primarily in the zonal mean component of the ENSO response. This is in contrast to the cold season (January-February-March) where the predictability of seasonal means over the Pacific/North American region is primarily in the wave component of the ENSO response.

Two modes dominate the variability of the mean JJA zonal mean height field. These modes are symmetric with respect to the equator. The first has maximum variance in the tropical upper troposphere, while the second has substantial variance in middle latitudes of both hemispheres. A regression analysis suggests that the first mode is forced by SST anomalies in the far eastern tropical Pacific and the Indian Ocean, while the second mode is forced by SST anomalies in the tropical Pacific extending eastward from the dateline.

The regression results concerning the forcing of the zonally symmetric modes were confirmed by an additional set of AGCM runs forced by idealized SST anomalies consisting of the 2 dominant JJA SST EOFs. By forcing the model with EOF 1 we were able to reproduce the height field anomalies determined from our analysis of the DSP results. Similarly for the second SST EOF. The impact of the zonally symmetric response on JJA precipitation in the middle latitudes

appears be weak. A comparison with observations shows, however, a signature of the zonally symmetric modes that is consistent with the occurrence of dry and wet years over the United States. We hypothesize that these modes, while imposing only weak constraints on mid-latitude warm season continental-scale climates, may play a role in the long-term predilection for drought or pluvial conditions. This work is being carried out in collaboration with Arun Kumar from NCEP.

Predictability of the 1988 drought and 1993 floods in the United States

As mentioned above, for the JJA runs, the initial soil moisture for each ensemble was taken from the appropriate year of one of our 20-year AMIP runs described above. In particular, it is important to know that each member of a particular ensemble has the same initial soil moisture. Results from the 9-member DSP runs for JJA show that the SST anomalies appear to produce only marginally significant precipitation anomalies over the continental United States during 1980-1999. To analyze this further, the ensemble size was increased to 18 members for the two years with extreme hydrologic conditions: the 1988 drought and the 1993 floods. To test the sensitivity to soil moisture we generated another set of 18 members for each year, but with different initial soil moisture (taken from a different AMIP run). An analysis of these two sets of 18 runs (see figure 10a in comparison with a more predictable region over South America shown in figure 10b) suggests that the main predictable signal over the United States is associated with memory of the initial soil moisture anomalies that developed during the previous winter and spring (apparently as a result of the strong ENSO wave response during those seasons).

Long-term Variability

A preliminary analysis of two of the AMIP integrations for 1950-1999 shows that the model produces remarkably realistic modes of interannual variability of the seasonal mean (JFM) 200mb height field. For example, the model produces a very realistic ENSO mode, both in terms of its spatial structure and time evolution including a substantial decadal change in the late 1970s. In fact, the model reproduces the spatial structure of 7 of the first 8 modes of JFM interannual variability found in the NCEP/NCAR reanalysis.

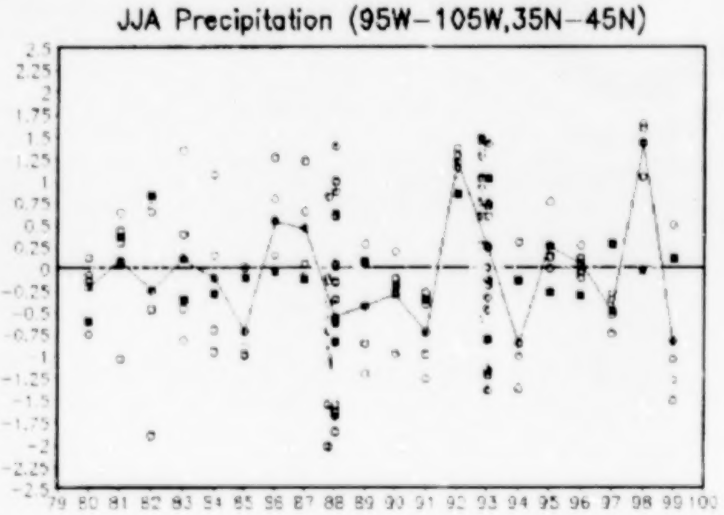

Figure 10a: A scatterplot of JJA precipitation in the U.S. Great Plains from NSIPP1 model hindcasts. Open circles are individual ensemble members. The line connects the ensemble means, blue squares are observations. For 1988 and 1993, two sets of 18 ensemble members (red and green circles) were generated, having different initial soil moisture.

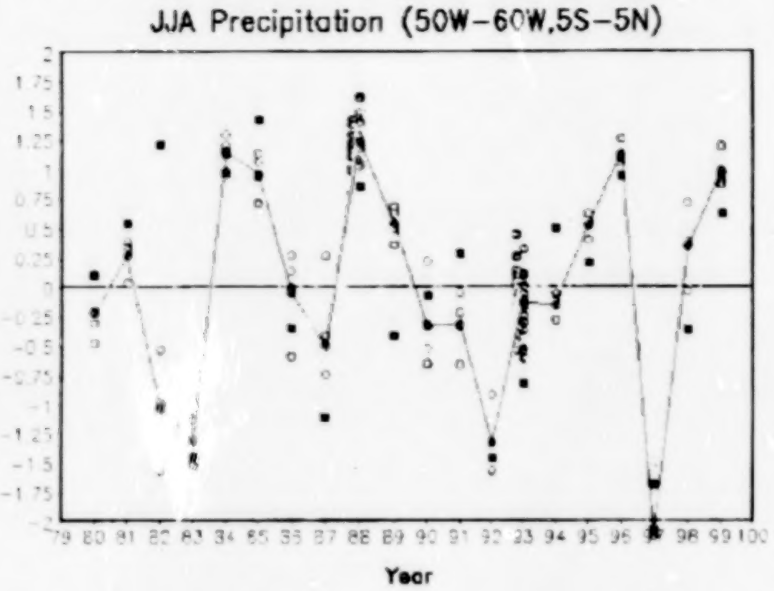

Figure 10b. Same as Figure 10a, except for a region over northern South America

4. Coupled AGCM-LSM Experiments

In an earlier study, we had examined the robustness of the NSIPP1 AGCM's response to prescribed moisture conditions at the land surface. The GCM was found to be strongly coupled to the land surface in transition zones between dry and humid regions. While this characterization of the NSIPP model's behavior is important in its own right, the study nevertheless left unanswered a critical question, namely, to what degree is the determined coupling strength model dependent? To address this question, a less computationally expensive version of the experiment was devised. A sixteen-member ensemble of two-month simulations was performed in which each member simulation was forced to maintain the same (geographically-varying) time series of land surface prognostic states. Coupling strength is quantified by examining the variation of precipitation amongst the ensemble members. (If, for example, all member simulations tend to produce roughly the same precipitation anomaly on the same day at a given cell, then the land-atmosphere coupling strength at that cell is considered high.) This experimental approach has been distributed to a number of climate modeling groups in the community, and so far two other groups have performed the experiment. A preliminary comparison of the three completed experiments suggests that the coupling strength in the NSIPP model is relatively high.

How can we determine if the NSIPP model's high coupling strength is realistic? A second coupled land-atmosphere experiment, currently in production, starts to address this. In this so-called "LDAS-style" experiment, the AGCM's precipitation is not allowed to fall on the land surface; instead, the land surface model is forced with precipitation from an observational dataset. As a result, the land surface during the run attains soil moistures and thus evaporation rates that are presumably more realistic than those that would be attained in a standard coupled land-atmosphere run. If precipitation is significantly controlled by land surface conditions, then the precipitation generated in the run (i.e., the precipitation that is not allowed to fall on the land surface) will also be more realistic. The preliminary results in Figure 11 show that this is indeed the case.

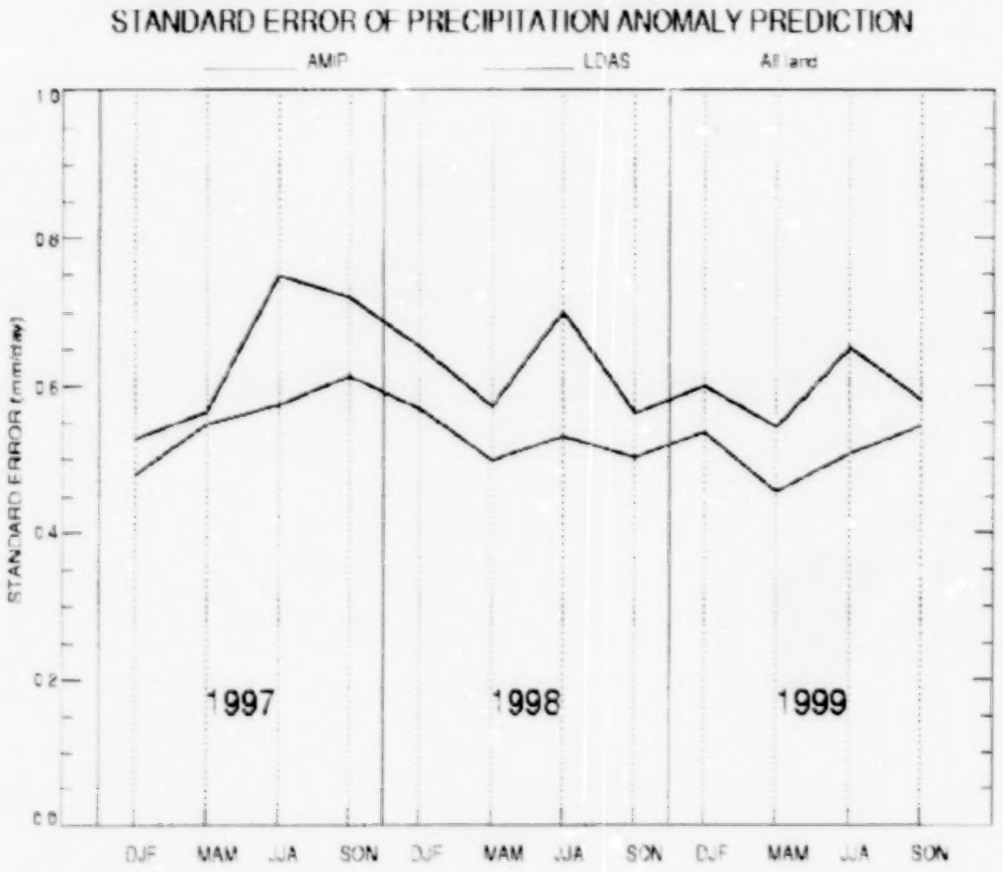

Figure 11. Standard error (relative to observations) of precipitation anomaly generation, as determined from a standard "AMIP-style" run (for which only realistic SSTs are imposed) and from an "LDAS-style" run (for which realistic SSTs are imposed and presumably realistic soil moisture conditions are maintained).

Shown are the standard errors of seasonal precipitation anomaly generation for the run with the presumably realistic soil moisture and for a standard AMIP-style run. The former has the smaller error, suggesting that precipitation generation in the real world is indeed partly controlled by land surface moisture conditions.

The predictability of precipitation will be addressed in the next phase of the second experiment described above, in which soil moisture states generated in the run (i.e., those generated under observed precipitation forcing) serve as initial conditions for forecasts. The predictability of soil moisture itself was the focus of a study recently submitted for publication in the Journal of Hydrometeorology. In this study, water balance considerations at the soil surface were used to derive an equation relating the autocorrelation of soil moisture in a climate model to four physical controls: (1) seasonality in the statistics of the atmospheric forcing, (2) the variation of evaporation with soil moisture, (3) the variation of runoff with soil moisture, and (4) persistence in the atmospheric forcing, as perhaps induced by land-atmosphere feedback.

As shown in Figure 12, the equation successfully captures the large-scale structure of the global autocorrelation field. We can thus use the four noted controls to explain why some regions have a stronger soil moisture memory (and thus might have a stronger potential for precipitation prediction) than other regions.

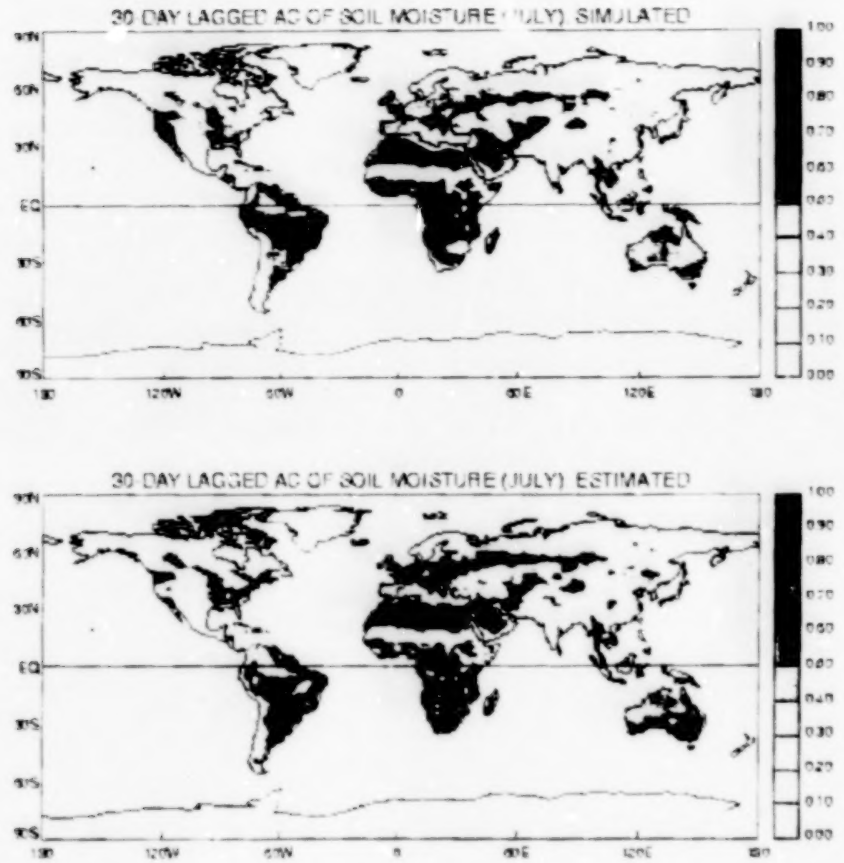

Figure 12. Top: Map of 30-day lagged autocorrelation of root zone soil moisture as determined from an ensemble of GCM simulations. Bottom: Corresponding map of 30-day lagged autocorrelation as estimated with the equation mentioned in the text.

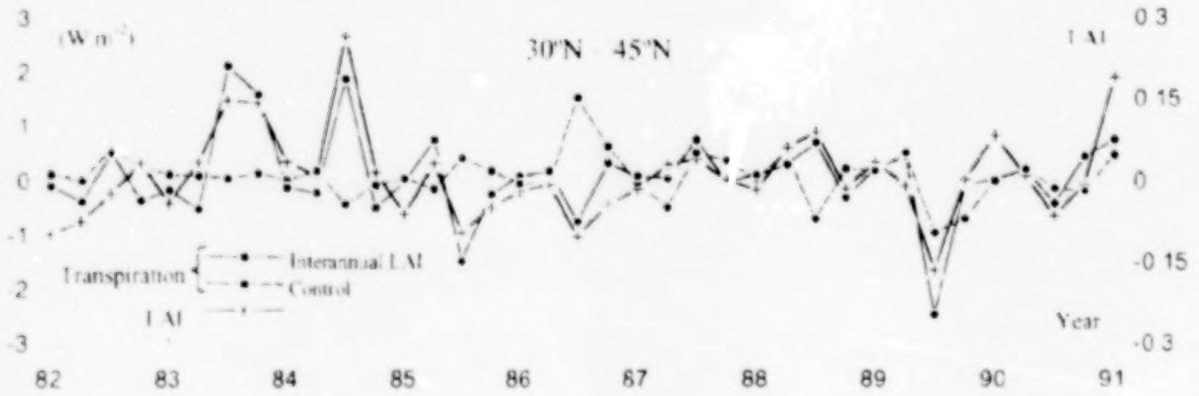

Figure 13. Satellite-derived seasonal anomalies of leaf area index (LAI) plotted against transpiration anomalies from both an "interannual LAI" simulation (in which the interannually varying LAI values are imposed at the land surface) and a "control simulation" (in which the mean seasonal cycle of LAI is imposed instead).

Finally, to examine how interannual variations in vegetation phenology affect simulated climate two parallel nine-year simulations have been carried out. In one of these simulations, vegetation leaf area index (LAI) and greenness fraction were given realistic interannual variations (from a dataset derived by Code 920 scientists from NDVI variations). In the other, the mean seasonal cycles of LAI and greenness fraction were prescribed each year. A preliminary comparison of the two runs suggests that on the regional scale, the impact of vegetation variability on evaporation and precipitation is largely drowned out by the larger impact of the atmospheric circulation's variability. Over broad latitudinal bands, however, we see some evidence of vegetation impact, as shown in Figure 13. These experiments, which must still be extended, start to address the usefulness of modeling interannual variability in vegetation phenology.

5. Ocean Data Assimilation

5.1 A Hierarchy of Systems

NSIPP is currently testing three ocean data assimilation systems (ODAS), each with increasing degrees of sophistication in the sequential estimation hierarchy. The three systems are univariate optimal interpolation (UOI), multivariate optimal interpolation (MvOI), and the ensemble Kalman filter (EnKF). For the UOI, only temperature data are assimilated and only temperature is corrected directly by the assimilation procedure. For the MvOI, all components of the ocean state (temperature, salinity, currents, sea surface height) are corrected directly by the assimilation even if a single variable, such as temperature or sea surface height, is assimilated. For the MvOI, the error statistics, both level of error variance and structure of covariances, remain fixed throughout the assimilation cycle. The error statistics for the MvOI have been estimated from a single snapshot of an ensemble of ocean runs. In contrast, the EnKF uses the evolving spread of an ensemble of ocean states to estimate the evolving multivariate error statistics.

The UOI currently used to produce the initial ocean state for the NSIPP coupled assumes that the forecast temperature error covariances are approximately Gaussian. Due to the high-resolution coverage and accuracy of the TAO measurements, the UOI appears to be effective in improving surface and sub-surface temperature-field estimates in the equatorial region in comparison with estimates without temperature assimilation. As a result, the introduction of the UOI into the coupled forecast system has resulted in significant improvements in the coupled model's hindcast skill of Niño3 temperature anomalies. Meanwhile, we continue to refine and validate our multivariate ODAS. A major improvement in the MvOI and EnKF has been the introduction of an algorithm to filter spurious long-range information from the background error. These spurious long-range covariances result from the small ensemble sizes used. In the filtering algorithm, the resulting background covariances have local compact support. This compact support has the added advantage of facilitating the parallel implementation of the ODAS.

5.2 MvOI Tests

Testing of the MvOI to date has concentrated on the Pacific Basin. Assimilation tests have been conducted using the TAO temperature profiles, with the focus on how the multivariate statistics improve the other fields, viz., salinity and currents. Comparisons of control simulations (i.e., without any data assimilation) with the UOI, and with the MvOI have been conducted for data spanning 1996 to 1998. All runs have been forced with daily surface winds from Atlas's SSMI analysis, and monthly mean precipitation from Xie-Arkin. The basis for comparison has been

observational analyses by Greg Johnson at PMEL. A comparison for a section across the equator at 155°W is shown in Figure 14. The UOI assimilation without any correction of the salinity field leads to an erroneous representation of salinity at all sections along the equator, with degradation in the salinity structure even compared with the control. This is ameliorated substantially with the MvOI, which also improves upon the control. A modified version of the UOI is shown in the figure. The modification attempts to retain the water mass structure present in the control simulation. This modification is currently undergoing further test in the forecast initialization as an approach that allows continuous assimilation for many years rather than the monthly restart of the assimilation that is currently needed.

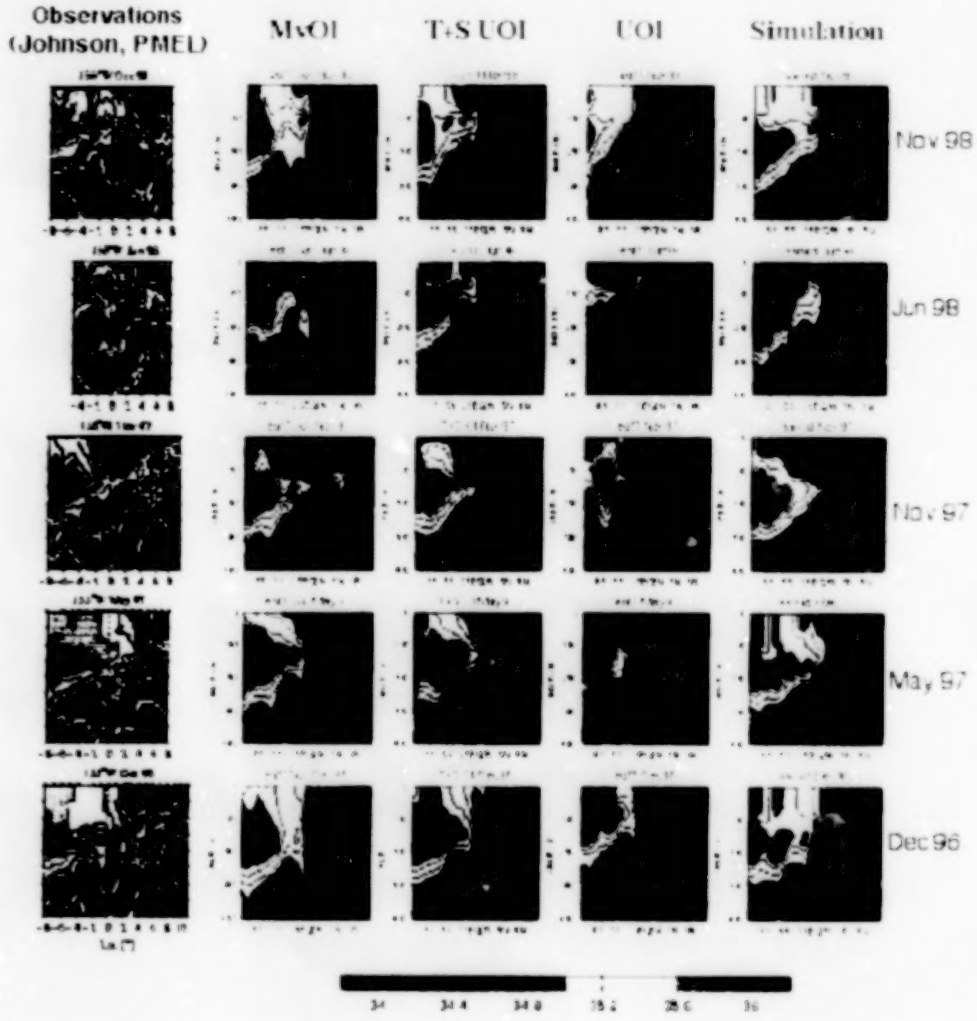

Figure 14: Monthly-mean salinity across the equator at 155°W using different covariance assumptions in the assimilation of TAO temperature profiles. The sections are from continuous assimilation begun in January, 1996. The time periods chosen for comparison coincide with the times of observation-only analyses from Johnson at PMEL. Note that the observations are not synoptic and are from single transects.

5.3 Ensemble Kalman Filter Tests

Keppenne and Rienecker (2001) compares the EnKF and UOI in the context of assimilating TAO temperature data. The experiment consists in using the EnKF to assimilate data into the 20-layer Pacific Basin version of Poseidon for three months starting January 1, 1993. Forty ensemble members were used and TAO temperature data assimilated every five days. Climatological forcing fields were combined with interannual wind-stress anomalies from an ensemble integration of the Aries atmospheric model. The purpose of the ensemble anomalies is to model the forcing errors. Model errors are ignored at this point. During the EnKF run, we rely on the central forecast (ensemble member closest to the ensemble) to estimate the true ocean state.

Along with the EnKF run, a control run without assimilation was initialized with the state of the ensemble central forecast at the beginning of the experiment and run for three months forced with climatological data. A third run in which the TAO temperature data were assimilated into Poseidon using the UOI assimilation algorithm was started from the same initial condition and used the same climatological forcing as the no-assimilation control run. Climatological forcing was used for convenience in this experiment but nothing precludes us from substituting the climatological fields with observed forcing fields.

The ocean states from the control and UOI-assimilation runs were compared with the central forecast from the EnKF run and with PMEL's TAO temperature analyses. Acoustic Doppler current profiler (ADCP) data and gridded satellite altimeter data from TOPLX/Poseidon were also used in cross-validation. Observed temperature anomalies from TAO serve to validate the year-long hindcasts.

Figure 15 shows the monthly mean temperature field along the equator for March 1993 in the case of the control, UOI-assimilation and EnKF-assimilation runs, and the corresponding field from the PMEL analyses. In the control, the thermocline is too deep to the West and too shallow to the East, as can be seen by examining the 20°C isotherm. The surface waters in the warm pool are also too warm, as examination of the 28°C isotherm reveals. The Equatorial temperature field from the UOI run is closer to the PMEL analysis in terms of the depth of the 20°C isotherm. However, the 28°C isotherm is split at the surface near 150E. In contrast, the multivariate EnKF analyses result in a temperature field that is significantly smoother than that produced with the UOI analyses. It also resembles the observations more closely than those from the control and UOI runs, as evidenced by the depths of the 20°C and 28°C isotherms in the central forecast of the EnKF run.

The evolution of the spatial-mean temperature anomaly with respect to the TAO climatology between 8°N and 8°S over the duration of the three-month assimilation and twelve-month hindcast periods is shown in Figure 16 for the control, UOI and EnKF runs. The corresponding spatial-mean anomaly from TAO is also shown. The significant forecast-model bias in the absence of assimilation is evident, as the control is initially about 0.5°C too warm and remains too warm until the end of the hindcast period. The UOI and EnKF analysis procedures both correct the model bias during the assimilation period. Once the hindcast starts, the UOI and EnKF temperature anomalies become warmer than the observations and start drifting back to the same level of excess seen in the anomalies from the control run. At least in the case of this experiment, the EnKF-run anomalies stay closer to the observed anomalies than the UOI-run

anomalies. A more in-depth analysis of the results reveals that the multivariate nature of the EnKF analysis is largely responsible for the improvement in hindcast skill with respect to that obtained when the data are assimilated using the UOI.

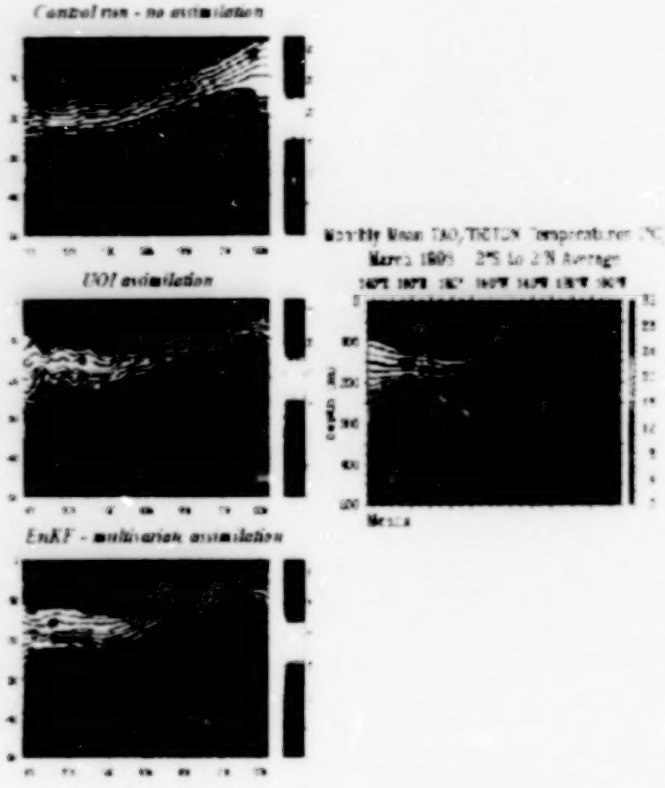

Figure 15. The monthly mean temperature field along the equator for March 1993 in the case of the control, UOI-assimilation and EnKF-assimilation runs, and the corresponding field from the PMEL analyses.

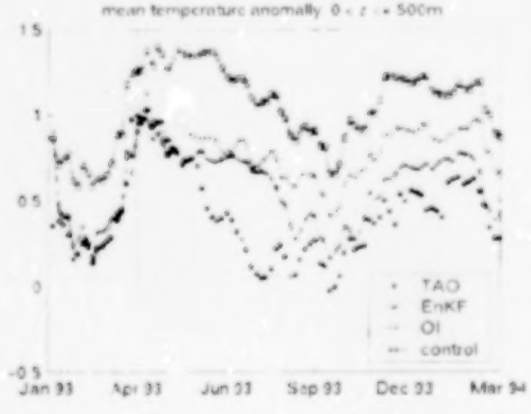

Figure 16. The timeseries of the spatial-mean temperature anomaly with respect to the TAO climatology between 8°N and 8°S over the duration of the three-month assimilation and 12-month hindcast periods.

A cross-validation of assimilation analyses is provided by comparison with ADCP derived currents at the TAO moorings (Figure 17). These data have not been assimilated into the analyses. At 170°W, the control and UOI runs severely underestimate the strength of the

Equatorial undercurrent which, at this longitude, flows at a depth of about 200m. The Equatorial-undercurrent strength from the EnKF run is closer to the observed strength. Moreover, in the UOI run, the undercurrent strength goes to zero and then becomes negative during the second half of March 1993. Again, we suspect that this deficiency of the UOI is due to the univariate assimilation methodology that updates the temperature field without modifying the salinity and current fields. At 140°W, the observed undercurrent strength at a depth of about 120m weakens during February 1993 and then returns to its January level during the third month of the experiment. The control run completely misses these amplitude changes. Both the EnKF and UOI runs show a behavior similar to that seen in the observations, but the current strength from the EnKF run resembles the observations more closely than that from the UOI run. These results, as well as those referring to the ADCP current data at 170°W, demonstrate the importance of using a multivariate assimilation methodology such as that used in the NSIPP ODAS which relies on cross-field covariances to update the model salinity and currents when temperature data are assimilated.

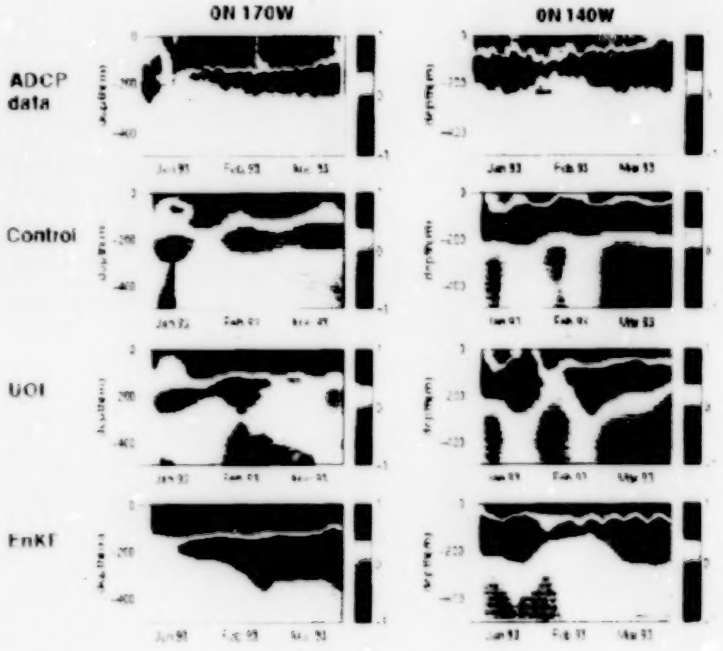

Figure 17. The top two panels show time-depth contour plots of the zonal current observations at two TAO moorings (left hand: 0°N, 170°W; right hand: 0°N, 140°W) equipped with ADCP current profilers during the three-month assimilation experiments. The two second-row panels show the corresponding time-depth contour plots from the control run. The third and fourth rows correspond to the UOI and EnKF runs, respectively.

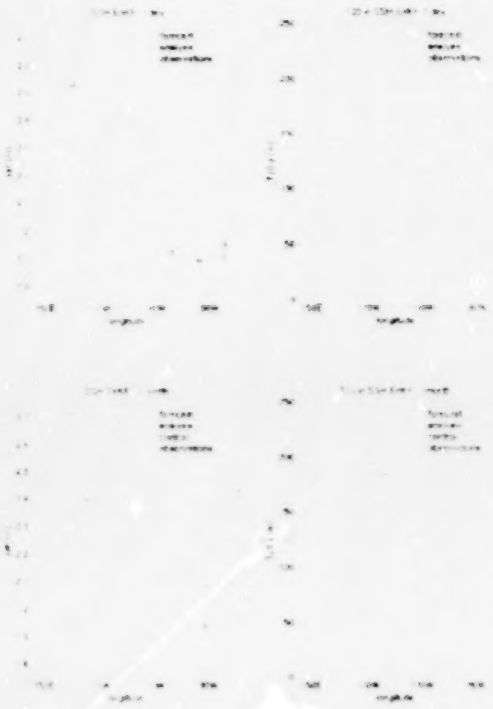

Figure 18. The SSH forecast along the Equator (central forecast [illegible] or to the first analysis one day into the experiment, upper panel, and after 1 month of assimilation, lower panel) is indicated by the solid blue line. The dashed red line corresponds to the analysis resulting from the assimilation of the TOPEX altimetry data identified by the green squares in the left hand panels. The right hand panels show the depth of the 20°C isotherm along the Equator in the forecast (solid blue line) and analysis (dashed red line). The green squares in the right hand panels show the depth of the 20°C isotherm computed from TAO temperature observations.

5.4 Results From the Multivariate Assimilation of Satellite Altimetry

Although most of our efforts so far have dealt with the assimilation of *in situ* TAO temperature data, one of the main justifications for the development of the NSIPP multivariate ODAS is for the assimilation of surface altimetric measurements. Initial experiments to assimilate Topex/Poseidon altimetric data have begun. In the experiment discussed here, gridded data were assimilated every five days for three months. The results are presented in Figure 18. The analysis does a very good job at reproducing the features present in the data. In addition to the SSH, the depth of the 20°C isotherm computed from TAO temperature observations is shown for comparison. The latter data are used for verification but are not assimilated. In the Western Pacific where the forecast 20°C isotherm depth is too shallow, the analysis tends to deepen the thermocline. In the Eastern Pacific where the forecast resembles the observations more than to the West, there is little difference between the forecast and analysis.

After one month, the SSH from the control run is severely underestimated. In contrast, for the EnKF run, the forecast and analysis are both close to the assimilated data. The fact that the forecast resembles the data indicates that the model layer thicknesses have changed consistently with the fact that the model SSH, which is computed from these thicknesses, is steered toward the TOPEX observations. There is also little change between the forecast and analysis for the 20°C isotherm depth shown in the lower right panel. In the Western Pacific, both are right on track. In the Eastern Pacific, they both overestimate the 20°C isotherm depth. The control on

the other hand underestimates the 20°C isotherm depth to the East as well as to the West. These results are encouraging, as they show that the assimilation of altimetry using the multivariate assimilation methodology not only improves the layer thickness, but also has the potential to correct errors present in the model prognostic fields when no SSH data are assimilated.

6. Land Data Assimilation

The framework for initializing soil moisture conditions in a forecast has advanced considerably through the efforts of Science Team members Paul Houser and Jeff Walker. A peer reviewed paper on the associated algorithm development and a synthetic study of assimilating near surface soil moisture observations into the NSIPP Catchment LSM has been submitted to the Journal of Geophysical Research. The requirements of a soil moisture measurement mission, including accuracy, repeat time and spatial resolution, are currently being examined. Assimilation of SMMR soil moisture data, as processed by Manfred Owe of Code 974, will begin in the near future. In collaboration with Paul and Jeff, we have started the transition of their system into the NSIPP production software suite.

7. Other Investigations

7.1 Subtropical-Tropical Ocean Exchanges

One of the potential contributors to decadal variability of the ENSO cycle is variability in the transport or water-mass properties of the exchange between subtropical and tropical gyres. The water masses which comprise the Equatorial Undercurrent (EUC) have their properties set at the surface in the northern and southern subtropical gyres. Changes in the intergyre exchange rate, or in the temperature of the EUC water masses may influence equatorial air-sea interaction, and feedback into ENSO dynamics.

The mechanics of this exchange process are poorly understood. Using the Poseidon OGCM and MICOM, another isopycnal model, we have been investigating the exchange pathways, transport, and seasonal variability in the northern hemisphere. Both models simulate both interior basin and western boundary current pathways similar to those seen in large scale climatological observational datasets. The models, however, show pronounced seasonality to the interior exchange in particular, with little cross gyre exchange in the thermocline during the boreal warm season, and strong exchange during the winter months. The seasonal variability is mediated by changes in the structure of the thermocline associated with seasonal variability in the wind and buoyancy forcing at the ITCZ. The variability of the interior exchange, which is a relatively insignificant source of water on an annual basis (2-5 Sverdrups), may act as a more significant influence on the EUC when the flux is concentrated within a 4-6 month period and over a localized region centered on 160°W. These results are described in Coles and Rienecker (2001).

Further investigations of the role of the subtropical cells have centered on understanding the role and source of subsurface salinity variability in the tropics. Much of the observed subsurface variability occurs in the thermocline, and may have its origin in the subtropics. Salinity acts both as a tracer of variability in the southern STC in particular, but is also crucial to the accurate assimilation of sea surface height variability into the ENSO forecasting system. Simulations of the decade from 1988-1998 show both ENSO timescale variability in the subsurface equatorial

and tropical salinity distributions (which compare well with observations), but also a trend in the southern subtropical thermocline salinity which has been observed at 165°E. The equatorial salinity structure in the model is closely coupled to zonal advection in the EUC, and to the surface wind stress, suggesting that as an essentially wind-driven process, it may be straightforward to simulate it in models with reasonable initial conditions. Investigations of the role of the long term salinity variability in influencing the thermal structure in the EUC are ongoing.

7.2 ENSO Dynamics

A numerical hindcast of the equatorial Pacific ocean circulation was conducted for the period of 1989-98 using the Poseidon quasi-isopycnal ocean model coupled to an atmospheric mixed layer model to study the ocean dynamics during the ENSO. The simulated results were compared with TOGA-TAO mooring measurements. The comparison indicates that the model is capable of reproducing the observed variations of the zonal velocity at seasonal-to-interannual time scales. The hindcast produced a sharp ocean thermocline with the speed of the Equatorial Undercurrent close to the observed. The interannual anomalies of the thermocline depth track the 20°C isotherm depth anomalies in the TAO data well and the model dynamic height is in good agreement with tide-gauge sea level and satellite altimetric data. The model sea surface temperature variations are highly coherent with the observed at periods longer than a season. The mean errors are generally less than 1°C. However, the variations can deviate from the TAO mooring observations by 1.5 - 2.0°C in the western Pacific warm pool and by larger than 3°C in the eastern equatorial Pacific cold tongue.

Based on the comparisons, the dynamics of the ENSO events in the 1990s were investigated in light of the existing ENSO paradigms. The investigation suggests that the Delayed Oscillator paradigm played an important role in the termination of the 1991-93 and the 1997/98 El Niño. The same paradigm does not explain the termination of the 1988/89 and the 1995-97 La Niña events well. The thermocline changes are consistent with the recharge paradigm except for the termination of the 1988/89 La Niña and the beginning of the 1991-93 El Niño. The Wyrtki paradigm is validated with the 1997/98 El Niño but is inconsistent with the 1991-93 El Niño. Reflected Rossby waves from the Pacific eastern boundary pushed the eastern edge of the warm pool back to the west during the termination of the El Niño. However, their roles are dwarfed by the signals from the western boundary at a later time. They did not appear to play an important role during the termination of the La Niña events. Our simulation suggests that the Western Pacific Oscillator proposed by Weisberg and Wang (1997) is not the primary process that controls the El Niño evolution in the 1990s. The balance between the windstress and the integrated zonal pressure gradient above the thermocline is found to prevail during normal years and has been greatly disrupted during the 1997/98 El Niño, suggesting that the slow "SST mode" of Neelin (1991) is not the major process in operation during the 1997/98 El Niño. A low frequency oscillation in the western Pacific sea levels is identified in the hindcast and is confirmed by the tide gauge observations. These results are described in Yuan et al. (2001).

7.3 Atmospheric Equatorial Momentum Budget

An analysis of the equatorial momentum budget in the NSIPP1 AGCM has been conducted. One of the main findings of this analysis is that the nature of the force balance in the equatorial marine boundary layer depends on the time scale of interest. The main balance in the boundary

layer is always between pressure gradient force and surface stress. However, seasonal variations in the boundary layer pressure force appear to result principally from shallow turbulent heating, while annual means and interannual variations in the pressure force are driven by deep free-tropospheric modes. We believe these modes to be connected to deep convective heating. We compared the force balances in the NSIPP1 AGCM with those found in the NCEP/NCAR reanalysis and found general agreement. These results are fully described in Bacmeister and Suarez (2001a,b).

8. Model Development

8.1 AGCM Development

An updated version of the NSIPP atmospheric general circulation model (AGCM) has been finalized, evaluated and documented (Bacmeister et al., 2000). The updated version of the model identified as the NSIPP1 AGCM features increased vertical resolution below 700 mbar, filtered topography, and minor modifications to the cumulus, large-scale cloud, and boundary-layer parameterization schemes. Major improvements over the earlier version of the AGCM include:

-Better simulation of wintertime, northern-hemisphere, stationary planetary waves, both in their multi-year mean and in their ENSO-related interannual variability.

-Better simulation of tropical precipitation; in particular the model's tendency to form "double-ITCZs" during most of the year has been largely eliminated

-Better simulation of surface wind stresses over the tropical Pacific, in both the annual mean and seasonal cycle.

An atlas of seasonal mean quantities from a 20-year (1979-1999) simulation using the NSIPP1 AGCM is presented in Bacmeister et al. (2000).

The improvements in simulated wind stress are particularly significant for coupled ocean/atmosphere simulations. Numerous free-running coupled simulations using the NSIPP1 AGCM were performed during the past year. These showed a significant improvement in the simulated annual cycle of SSTs in the eastern equatorial Pacific over that obtained with the previous version of the AGCM.

The polar filter of the NSIPP1 AGCM has been modified for use with a variable-resolution grid. The model's dynamical core uses a polar filter to control the linear instability due to the convergence of the meridians at the poles. Since the original Fourier filter is not appropriate for use with a stretched-grid, an alternative filtering technique, using a convolution filter developed by Takacs et al. (1999) has been added to the NSIPP1 AGCM. It has eliminated the small-scale noise that was produced by the Fourier filter in the regions of highest longitudinal resolution near the poles. This filter has proved essential for the feasibility of simulations on stretched grids that are strongly stretched such as the grid that has a quarter of a degree resolution over the Amazon Basin and gradually stretches to 4 degrees at the antipodal point (hereafter referred to as Stretched 0.25-to-4).

This regional version of the NSIPP1 model was used to perform Austral Summer season simulations with various stretched grid configurations (Stretched 1-to-4, 0.5-to4, and 0.25-to-4). The NSIPP1 regional climate model preserves global integrity of atmospheric circulations and precipitation well. The model's representation of interannual variability is also very comparable to that of its uniform grid counterpart.

The NSIPP1 AGCM works well on a stretched grid and therefore can be a useful tool for studying two-way interacting regional climate. The new convolution polar filter allows strong stretching and enhances cost effectiveness while maintaining the global integrity of the simulations.

8.2 LSM Development

This year has seen the publication of two papers (Koster et al., 2000; Ducharne et al., 2000) describing the NSIPP Catchment land surface model (LSM) and the acceptance of a paper describing the snow model. The snow model of Lynch-Stieglitz (1994) has been coupled to the global catchment LSM (Stieglitz et al., 2001). This three-layer snow model accounts for snow melting and refreezing, dynamic changes in snow density, snow insulating properties, and other physics relevant to the growth and ablation of the snowpack. Validation with 1987-1988 ISLSCP data sets over the 5000 catchments representing North America indicates that the model is capable of simulating the spatial coverage of snow realistically. More importantly, the model's treatment of the insulation properties of snow cover leads to an accurate simulation of the permafrost front, relative to the NSIDC digital permafrost map. Finally, the successful larger-scale application of the model for North America suggests that the global application of the model is within reach, and more specifically, that application at high latitudes will be successful. These models (coupled together) are being tested offline in the Torne/Kaliz River system in northern Scandinavia, as part of the PILPS2E project.

Model development has focused in part on the improvement of a physically-based photosynthesis and stomatal conductance parameterization and its integration into the Mosaic LSM. (The integration into the NSIPP Catchment LSM will be equivalent.) The scheme describes the simultaneous transfer of CO_2 and water vapor into and out of the leaf through stomatal control. The scheme is being developed in collaboration with Jim Collatz of Code 923, who is also formulating a model of dynamic vegetation phenology. Our long-term plans are to use the dynamic vegetation model to track vegetation state as well as soil moisture conditions during seasonal forecasts.

References

Bacmeister, J. T. and M. J. Suarez, Wind-stress simulations and equatorial dynamics in an AGCM Part I: Basic results from a 1979-1999 forced SST experiment, *J. Atmos. Sci.*, (submitted), 2001a.

Bacmeister, J. T. and M. J. Suarez, Wind-stress simulations and equatorial dynamics in an AGCM Part II: Equatorial momentum budget and its relation to oceanic wind stress, *J. Atmos. Sci.*, (submitted), 2001b.

Bacmeister, J. T., P. J. Pegion, S. D. Schubert, and M. J. Suarez, Atlas of seasonal means simulated by the NSIPP1 atmospheric GCM, NASA Technical Memorandum 104606, V17, 194pp, 2000.

Chang, Y., S. D. Schubert and M. J. Suarez, Boreal winter predictions with the GEOS-2 GCM. The role of boundary forcing and initial conditions. *Quart. J. Roy. Met.Soc.* 126, 1-29, 2000.

Ducharne, A., R. D. Koster, M. J. Suarez, M. Stieglitz, and P. Kumar, A catchment-based approach to modeling land surface processes in a GCM, Part 2, Parameter estimation and model demonstration, *J. Geophys. Res.*, 105, 24823-24838, 2000.

Keppenne C. L. and M. M. Rienecker: Implementation and validation of a parallel ensemble Kalman filter for a high-resolution isopycnal Pacific Ocean circulation model (draft ms), 2001.

Koster, R. D., M. J. Suarez, A. Ducharne, M. Stieglitz, and P. Kumar, A catchment-based approach to modeling land surface processes in a GCM, Part 1, Model Structure, *J. Geophys. Res.*, 105, 24809-24822, 2000.

Lynch-Stieglitz, M., The development and validation of a simple snow model for the GISS GCM, *J.Clim.*, 7, 1842-1855, 1994.

Neelin, J. D., The slow sea surface temperature mode and the fast-wave limit: Analytic theory for tropical interannual oscillations and experiments in a hybrid coupled model, *J. Atmos. Sci.*, 48, 584-606, 1991.

Pegion, P., S. Schubert, and M. J. Suarez, An Assessment of the Predictability of Northern Winter Seasonal Means with the NSIPP1 AGCM. NASA Tech Memo. 104606, V18, 110 pp, 2000.

Stieglitz, M., A. Ducharne, R. D. Koster, and M. J. Suarez, The impact of detailed snow physics on the simulation of snow cover and subsurface thermodynamics at continental scales, *J. Hydromet.* (in press), 2001.

Takacs, L., W. Sawyer, M. Suarez, and M. S. Fox-Rabinowitz, Filtering techniques on a stretched grid general circulation model. Technical Report Series on Global Modeling and Data Assimilation, NASA/TM-1999-104606, Vol. 16, 1999.

Weisberg, R.H. and C. Wang, A Western Pacific Oscillator Paradigm for the El Niño-Southern Oscillation, *Geophys. Res. Lett.*, 24, 779-782, 1997.

NSIPP Personnel

GSFC Civil Servants
David Adamec (Code 971)
Jim Hansen (Code 940)
Randy Koster (Code 974)
Michele Rienecker (Code 971)
Siegfried Schubert (Code 910.3)
Max Suarez (Code 913)

Research Scientists
Julio Bacmeister (Code 913, GEST)
Victoria Coles (Code 971, GEST)
Pierre Guillevic (Code 974, GEST)
Christian Keppenne (Code 971, GSC)
Sarith Mahanama (Code 974, GEST)
Rosana Nieto Ferreira (Code 913, GEST)
Rolf Reichle (Code 974, GEST)
Alberto Troccoli (Code 971, GEST)
Augustin Vintzileos (Code 971, GEST)
Dongliang Yuan (Code 971, GEST)

Research Assistants
Anna Borovikov (Code 971, GSC)
Michael Kistler (Code 913, GSC)
Sonya Miller (Code 971, GSC)
Philip Pegion (Code 913, GSC)
Lori Tyahla (Code 974, GSC)
John Waldrop (Code 971, GSC)

System Administrator
Richard Mollel (Code 971, GSC)

Administrative Assistant
Nefertari Johnson (Code 971, GSC)

NSIPP Publications, 2000

Refereed

Bacmeister, J. T. and **M. J. Suarez**, Wind-stress simulations and equatorial dynamics in an AGCM Part I: Basic results from a 1979-1999 forced SST experiment, *J. Atmos. Sci.*, (submitted), 2001a.

Bacmeister, J. T. and **M. J. Suarez**, Wind-stress simulations and equatorial dynamics in an AGCM Part II: Equatorial momentum budget and its relation to oceanic wind stress, *J. Atmos. Sci.*, (submitted), 2001b.

Borovikov, A., M. M. Rienecker, and P.S. Schopf, Surface heat balance in the Equatorial Pacific Ocean: Climatology and the warming event of 1994-95, *J. Climate*, 14, 2624-2641, 2001.

Chang, Y., **S. D. Schubert** and **M. J. Suarez**, Boreal winter predictions with the GEOS-2 GCM: The role of boundary forcing and initial conditions. *Quart. J. Roy. Met.Soc.* 126, 1-29, 2000.

Coles, V., and **M. M. Rienecker**, North Pacific subtropical-tropical gyre exchanges in the thermocline: Simulations with 2 isopycnic OGCM's, *J. Phys. Oceanogr.* (in press), 2001.

Dirmeyer, P. A., F. J. Zeng, A. Ducharne, J. Morrill, and **R. D. Koster**, The sensitivity of surface fluxes to soil water content in three land surface schemes, *J. Hydromet.*, 1, 121-134, 2000.

Ducharne, A., **R. D. Koster, M. J. Suarez**, M. Stieglitz, and P. Kumar, A catchment-based approach to modeling land surface processes in a GCM, Part 2, Parameter estimation and model demonstration, *J. Geophys. Res.*, 105, 24823-24838, 2000.

Keppenne C. L., Data assimilation into a primitive equation model using a parallel ensemble Kalman filter, *Mon. Wea. Rev.*, 128, 1971-1981, 2000.

Keppenne C. L. and **M. M. Rienecker**: Implementation and validation of a parallel ensemble Kalman filter for a high-resolution isopycnal Pacific Ocean circulation model (draft ms), 2001.

Koster, R. D., M. J. Suarez, A. Ducharne, M. Stieglitz, and P. Kumar, A catchment-based approach to modeling land surface processes in a GCM, Part 1, Model Structure, *J. Geophys. Res.*, 105, 24809-24822, 2000.

Koster, R. D., M. J. Suarez, and M. Heiser, Variance and predictability of precipitation at seasonal-to-interannual timescales, *J. Hydromet.*, 1, 26-46, 2000.

Koster, R. D., and **M. J. Suarez**, Soil moisture memory in climate models, *J. Hydromet.* (submitted), 2001.

Nieto Ferreira, R., M. J. Suarez, and S. Nigam, Idealized simulations of the effects of Amazon convection and baroclinic waves on the South Atlantic convergence zone, *J. Atmos. Sci.* (in revision) 2001.

Nogues Paegle, J., R. Fu, E. H. Berbery, W. Chao, Chen, K. Cook, Enfield, V. Kousky, B. Liebmann, K. Mo, D. Neelin, **R. Nieto Ferreira**, J. Paegle, Robertson, A. Seth, and J. Zhou, The South-American monsoon system: new perspectives and future challenges, *BAMS* (submitted), 2001.

Rickenbach, T. M., **R. Nieto Ferreira**, J. Halverson, and M. A. F. Silva Dias, Mesoscale properties of convection in Amazonia in the context of large-scale wind regimes, *J. Geophys. Res.* (in press), 2001.

Schubert, S. D., M. J. Suarez, Y. Chang, and G. Branstator, The impact of ENSO on extratropical low frequency noise in seasonal forecasts, *J. Climate*, 14, 2351-2365, 2001.

Schubert, S. D. and M. L. Wu, Predictability of the 1997 and 1998 south Asian summer monsoons, *J. Climate* (in press), 2001.

Schubert, S., M. J. Suarez, P. Pegion and **M. Kistler**, and A. Kumar, Predictability of Zonal Means During Boreal Summer, *J. Climate* (submitted), 2001.

Stieglitz, M., A. Ducharne, **R. D. Koster**, and **M. J. Suarez**, The impact of detailed snow physics on the simulation of snow cover and subsurface thermodynamics at continental scales, *J. Hydromet.* (in press), 2001.

Sud, Y. C., D. M. Mocko, G. K. Walker, and **R. D. Koster**, Influence of land-surface fluxes on precipitation: Inferences from simulations performed with ARM-CART SCM dataset, *Mon. Wea. Rev.* (submitted), 2001.

Yuan, D., M. M. Rienecker, and P. S. Schopf, A numerical hindcast of the Equatorial Pacific Ocean circulation in the 1990's, *J. Climate* (submitted), 2001.

Non-refereed

Bacmeister, J. T., P. J. Pegion, S. D. Schubert, and **M. J. Suarez**, Atlas of seasonal means simulated by the NSIPP1 atmospheric GCM, NASA Technical Memorandum 104606, 17, 194pp, 2000.

Bacmeister, J. and **M. J. Suarez**, Analysis of the momentum budget over the equatorial Pacific in an Atmospheric GCM. Proceedings of 25th Climate Diagnostics and Prediction Workshop, 2000.

Miller, S., M. J. Suarez, M. M. Rienecker, J. Bacmeister, D. Adamec, A. Vintzileos, and D. Waliser, NSIPP's Coupled Simulations: Climatologies and Interannual Variations in the Upper Ocean of the Tropical Pacific. Proceedings of 25th Climate Diagnostics and Prediction Workshop, 2000.

Pegion, P., S. Schubert, and **M. J. Suarez**, Seasonal (JFM) Predictability of the NSIPP1 AGCM. NASA Tech Memo. 104606, 2000.

Schubert, S., M. J. Suarez, and **P. Pegion**, Predictability of Seasonal Means in the NSIPP1 AGCM. Proceedings of 25th Climate Diagnostics and Prediction Workshop, 2000.

Vintzileos, A., M. M. Rienecker, M. J. Suarez, A. Borovikov, and **S. Miller**, Initialization shocks, drifts and adjustments of the NSIPP ENSO forecasting system. Proceedings of 25th Climate Diagnostics and Prediction Workshop, 2000.

Model Data Distribution

AGCM output distributed through www interface.

Michael Yan, GSFC, 5 requests, 3.45 GB *
Jack Ritchie, Scripps, 1 request, *
Baode Chen, GSFC, 5 requests, 2.13 GB *
Eric DeWeaver, University of Wash., 4 requests, 5.18 GB *
Andrew Mai, NCAR, 1 request, 4.83 GB
Grant Branstator, NCAR, 6 requests, 3.18 GB
J. Hernandez, GSFC, 1 request, 0.28 GB
Sam Iacobellis, Scripps, 3 requests, 0.20 GB
Michael Chen, Iowa State, 5 requests, 1.54 GB
Dan Fitzjarrald, MSFC, 1 request, 0.92 GB
Peter Robertson, MSFC, 1 request, 1.04GB
Jenny Wu, GSFC, 5 requests, 1.43 GB
Suzana Camargo, 2 requests, 46.10 GB

* Indicates one of four requests submitted before size records were kept; the count indicates these hits on the website, but the totals do not.

Totals: 40 requests, 70.28 GB
Average per request: 0.64GB (excluding Camargo request).

NSIPP Science Team

In November 1998 a Science Team of 8 funded collaborations was chosen from a competitive response to an Announcement of Opportunity to collaborate with and support the NSIPP core effort at Goddard. An introductory Science Team Meeting was held in May, 1999. Additional science team members were added from the GMAP NRA in 1999. The second Science team meeting was held July 11-12, 2000. NSIPP also funds collaborations essential to the core effort.

CGCM and AGCM Diagnostics

Grant Branstator, NCAR and M. Chen, Iowa State University, *Diagnosis and simulation of the South-east Asian-induced wavetrain that occurs during tropical Pacific cold and warm events.*

Sumant Nigam, University of Maryland, *Dynamical diagnosis of the NSIPP atmospheric and coupled model simulations.*

John Roads, Scripps Institution of Oceanography, *Seasonal and Atmospheric predictions.*

Chunzai Wang, NOAA/AOML/U. Miami, *Studies of western Pacific Interannual Anomaly patterns toward improved ENSO prediction.*

David Neelin, IGPP, UCLA, *Sensitivity of Precipitation in Coupled Land-Atmosphere models.*

Richard Kleeman, Courant Institute of Mathematical Sciences, NYU, *An investigation of the predictability of the NSIPP forecast system.*

Ping Chang and Ben Giese, TAMU, and R. Saravanan, NCAR, *Modeling Tropical Atlantic Variability.*

Land Surface Model Development and Land Assimilation

Paul Houser, GSFC, and Jay Famiglietti, University of Texas, *Optimal land initialization for seasonal climate predictions.*

Ocean data assimilation and coupled forecasting

Eugenia Kalnay, University of Maryland, *Ensemble ocean-atmosphere perturbations with growing ENSO modes using breeding.*

Thorsten Markus, JCET/GSFC/UMBC, *Improved Surface Heat and Salt Fluxes at polar latitudes through the assimilation of satellite measurements.*

Ocean Model Development

William Dewar, Florida State University, *Thermodynamics in layered models.*

NSIPP Associate Investigators

Paul Schopf, George Mason University, *Development of the Poseidon Ocean Model for NSIPP.*

Marc Stieglitz, Lamont Doherty Earth Observatory, *Land surface model development for NSIPP.*

END